Brief paper

Shortest Dubins paths through three points ☆

Zheng Chen [a,*], Tal Shima [b]

[a] *Zhejiang University, Hangzhou 310027, Zhejiang, China*
[b] *Technion — Israel Institute of Technology, Haifa 32000, Israel*

ARTICLE INFO

ABSTRACT

The 3-Point Dubins Problem (3PDP) consists of steering a Dubins vehicle through three consecutive points with prescribed heading orientations at initial and final points so that the resulting path is the shortest. Characterizing the path of the 3PDP is important because (1) it provides insightful views on the solution paths of the Dubins Traveling Salesman Problem (DTSP) and the Curvature-Constrained Shortest-Path Problem (CCSPP) as they are natural extensions of the 3PDP and (2) some algorithms in the literature for solving the DTSP and the CCSPP require efficient methods for solving the 3PDP. In this paper, Pontryagin's maximum principle is used to show that the path of 3PDP must lie in a sufficient family of 18 types. Moreover, a formula in terms of the parameters of the 3PDP for all the 18 types is established, and this formula reveals the relationship between the unknown orientation angle at mid point and known parameters. By observing that the formula can be converted into some polynomials, the 3PDP can therefore be efficiently solved by finding zeros of those polynomials. Finally, numerical simulations illustrate the developments by comparing with the straightforward discretization-based method.

1. Introduction

Missions for autonomous aerial and ground vehicles are usually planned based on a hierarchical architecture. The higher level of the architecture is about selecting and assigning targets to a vehicle; at the lower level, the vehicle orders the sequence of targets and routes a path visiting these targets with a minimum cost. If the vehicle can change its direction quickly relative to the distance between any two targets, the problem to be solved at the lower level can be described by the Traveling Salesman Problem (TSP) which, given a set of waypoints, consists of finding a shortest path that visits each waypoint exactly once and finally returns to the initial waypoint. When the cost between any two waypoints is defined by the Euclidean distance, the problem is dubbed the Euclidean TSP (ETSP).

Since some schemes have been available in Arora (1998), Lawler, Lenstra, Rinnooy Kan, and Shmoys (1985) to solve the ETSP with a complexity of $n \log(n)$ where n is the problem's size, the solution of ETSP has been widely applied to motion planning.

However, when a vehicle is subject to nonholonomic constraints, the solution from ETSP provides poor estimates for optimal paths. Since the Dubins vehicle (Dubins, 1957), moving only forward at a constant speed with a maximum curvature, provides an excellent kinematic prototype for nonholonomic vehicles such as unmanned aerial vehicles (Matveev, Teimoori, & Savkin, 2011), fixed-wing aircrafts (Lugo-Cárdenas, Flores, Salazar, & Lozano, 2014), and thrusted skates (Lynch, 2003), the TSP for Dubins vehicles (DTSP for abbreviation hereafter) has seen a wave of research interests in the past two decades.

Unlike the ETSP, solving the DTSP requires not only ordering the sequence of waypoints but also optimizing the vehicle's Heading Orientation Angle (HOA) at each waypoint; this results in another source of difficulty. Some genetic algorithms were employed in Edison and Shima (2011) and Yu and Hung (2012) to perform brute-force search for the global solution of DTSP. Nevertheless, it was proven in Ny, Feron, and Frazzoli (2012) that the DTSP was NP-hard, implying that solving the DTSP by brute-force optimization was hardly practical for the scenarios when the control decisions had to be made in situ or, if not exactly, at least efficiently. Due to this challenging issue, some heuristics are used to solve the DTSP. For example, a k-step Look-Ahead Algorithm (LAA) was proposed in Isaiah and Shima (2015) for the DTSP. More recently, the HOA at each waypoint was discretized in Cohen, Epstein and Shima (2017) to formulate an integer mathematical programming so that a standard solver was employed to solve the DTSP.

To approximate the solution of DTSP, a typical variant of the DTSP, that is the Curvature-Constrained Shortest-Path Problem (CCSPP) for which the sequence of waypoints is ordered in advance, is usually solved. Since the order of waypoints is fixed, the solution of CCSPP is a concatenation of the shortest Dubins paths between two configurations (a configuration consists of a position and a HOA) according to Bellman's principle for optimality (Bellman, 1957). Hence, solving the CCSPP amounts to selecting a sequence of HOAs so that the concatenated Dubins path is the shortest.

Some approximation-based algorithms have been proposed in the literature to select such HOAs for the CCSPP. In Salva, Frazzoli, and Bullo (2005), an alternating algorithm was proposed to approximate the HOAs. A linear-time approximation algorithm that computes a path whose length is within a constant factor of the optimal was proposed in Lee, Cheong, Kwon, Shin, and Chwa (2000). Based on the principle of receding horizon, some LAAs were developed in Cohen, Epstein, Isaiah, Kuzi and Shima (2017), Ma and Castanon (2006) and Rathinam, Sengupta, and Darbha (2007). In Rathinam et al. (2007), each HOA was designed by looking one target ahead. The 2-step LAA in Ma and Castanon (2006) is a natural extension since it looks two waypoints ahead. In Cohen, Epstein et al. (2017), a discretization-based LAA was proposed so that further waypoints could be taken into account.

Some researchers have recently used optimization techniques to generate the HOAs for the CCSPP. Once an optimization method is employed, the gradient information of the CCSPP with respect to its HOAs is usually required. While a numerical method was available in Tang and Özgüner (2005) to approximate the gradient, an analytical study was performed in Goaoc, Kim, and Lazard (2013) to present a set of analytical gradients under the assumption that the distance between any two consecutive points is at least four times of the vehicle's minimum turning radius. With this analytical gradient and the distance assumption, it was proven in Goaoc et al. (2013) that every CCSPP consisted of some convex sub-problems, and a standard convex algorithm could be used to solve the CCSPP; if the size n of the CCSPP is large, it is however impractical to solve by convex optimization since the number of sub-problems is up to 2^{n-2}. In a similar direction, the dynamic programming was applied in Takei and Tsai (2013) and Takei, Tsai, Shen, and Landa (2010) for the CCSPP.

In addition to the aforementioned optimization methods, the Coordinate Descent Algorithm (CDA), a mature optimization algorithm that successively minimizes over a coordinate hyperplane while fixing all other coordinates (Wright, 2015), was used to solve the CCSPP in Sadeghi and Smith (2016). Since the solution sequence generated by the CDA is nonincreasing, any solution obtained by approximation methods can be further improved by the CDA. Each step of the CDA is about optimizing a HOA at a waypoint while fixing HOAs at other waypoints; this is exactly solving a 3-Point Dubins Problem (3PDP), consisting of three waypoints with prescribed HOAs at initial and final waypoints. Hence, synthesizing the solution path of the 3PDP will significantly reduce the computational complexity of the CDA. In fact, the solution of the 3PDP have other applications. An immediate example is the discretization-based LAA (Cohen, Epstein et al., 2017) once over 3 targets are looked ahead. Another example is that, once a new point is inserted into a mission with minimum additional cost, the solution to a new 3PDP is required. In addition, synthesizing the solution of 3PDP gives insightful views on the solution paths of the DTSP and the CCSPP as they are natural extensions of the 3PDP.

Due to the significance of the 3PDP, it was studied in Goaoc et al. (2013), Ma and Castanon (2006), Rathinam and Khargonekar (2016) and Sadeghi and Smith (2016) with some relaxations or strict assumptions. Assuming that the distance between any two points is at least four times of the vehicle's minimum turning radius, the gradient of 3PDP with respect to the HOA at mid point was derived in Goaoc et al. (2013). Some relaxed versions of 3PDP were studied in Ma and Castanon (2006) and Rathinam and Khargonekar (2016). All the relaxations or assumptions in Goaoc et al. (2013), Ma and Castanon (2006), Rathinam and Khargonekar (2016) and Sadeghi and Smith (2016) aimed at restricting the solution in a narrow set so that the elementary geometry can be used to characterize the solution. For instance, with the same assumption of Goaoc et al. (2013), the inverse geometry was used in Sadeghi and Smith (2016) to design an iterative method for the 3PDP.

In the paper, the solution path of 3PDP will be characterized without any relaxations and assumptions. By using Pontryagin's maximum principle (Pontryagin, Boltyanski, Gamkrelidze, & Mishchenko, 1962), the solution path for any 3PDP is restricted into a family of 18 types. Moreover, a formula in terms of the parameters of the 3PDP is established for all the 18 types. This formula not only reveals the relationship of the parameters of 3PDP but also rules out a possible geometric property presented in Goaoc et al. (2013). In addition, the formula is converted to some polynomials so that the solution path of 3PDP can be efficiently solved by finding zeros of those polynomials. Some numerical examples are simulated finally to illustrate the developments presented in the paper.

2. Preliminary

In this section, the 3PDP is formulated and its necessary conditions are established.

2.1. Problem statement

For a Dubins vehicle moving only forward at a constant speed with a minimum turning radius, its configuration $\boldsymbol{x} := (x, y, \theta) \in \mathbb{R}^2 \times \mathbb{S}^1$ consists of a position vector $(x, y) \in \mathbb{R}^2$ and a HOA $\theta \in \mathbb{S}^1$. Without loss of generality, assume that the speed is one and the minimum turning radius is $\rho \in \mathbb{R}_+$. Then, the kinematics for the Dubins vehicle is given by

$$(\Sigma): \quad \frac{\mathrm{d}}{\mathrm{d}t} \begin{pmatrix} x(t) \\ y(t) \\ \theta(t) \end{pmatrix} = \begin{pmatrix} \cos\theta(t) \\ \sin\theta(t) \\ u(t)/\rho \end{pmatrix}$$

where $t \in \mathbb{R}_+$ is the time and $u \in [-1, 1]$ is the control. Throughout, whenever an individual 3PDP is mentioned, we refer to the following definition and notations.

Problem 1 (*3PDP*). Given three points $\boldsymbol{z}_1$, $\boldsymbol{z}_m$, and $\boldsymbol{z}_2$ in $\mathbb{R}^2$, let θ_1 and θ_2 in $[0, 2\pi)$ be the prescribed HOAs at $\boldsymbol{z}_1$ and $\boldsymbol{z}_2$, respectively. Then, the 3PDP consists of steering (Σ) by $u(\cdot) \in [-1, 1]$ on $[0, t_f]$ from $(\boldsymbol{z}_1, \theta_1)$, pathing $\boldsymbol{z}_m$ at $t_m \in (0, t_f)$, to $(\boldsymbol{z}_2, \theta_2)$ so that $t_f > 0$ is minimized.

As the vehicle's speed is a constant, solving the 3PDP is equivalent to finding the shortest path. Given any two configurations $(\boldsymbol{y}_1, \eta_1)$ and $(\boldsymbol{y}_2, \eta_2)$ in $\mathcal{X} := \mathbb{R}^2 \times \mathbb{S}^1$, denote by

$$F : \mathcal{X}^2 \to \mathbb{R}, \; [(\boldsymbol{y}_1, \eta_1), (\boldsymbol{y}_2, \eta_2)] \mapsto F[(\boldsymbol{y}_1, \eta_1), (\boldsymbol{y}_2, \eta_2)]$$

the length of the shortest Dubins path from $(\boldsymbol{y}_1, \eta_1)$ to $(\boldsymbol{y}_2, \eta_2)$. We denote the HOA at $\boldsymbol{z}_m$ along the path of 3PDP by $\theta_m \in [0, 2\pi)$, i.e.,

$$\theta_m := \underset{\theta \in [0, 2\pi)}{\operatorname{argmin}} F[(\boldsymbol{z}_1, \theta_1), (\boldsymbol{z}_m, \theta)] + F[(\boldsymbol{z}_m, \theta), (\boldsymbol{z}_2, \theta_2)].$$

In the next subsection, the necessary conditions for the 3PDP will be presented.

2.2. Necessary conditions

Denote the costate of $\boldsymbol{x} \in \mathcal{X}$ by $\boldsymbol{p} := [p_x, p_y, p_\theta]$ in cotangent space $T_{\boldsymbol{x}}^* \mathcal{X}$. According to Pontryagin's maximum principle (Pontryagin et al., 1962), if a trajectory $\boldsymbol{x}(\cdot) = [x(\cdot), y(\cdot), \theta(\cdot)]^T \in \mathcal{X}$ associated with a measurable control $u(\cdot) \in [-1, 1]$ on $[0, t_f]$ is the solution of 3PDP, there exists a scalar $p^0 \leq 0$ and a continuous mapping $t \mapsto \boldsymbol{p}(\cdot) \in T_{\boldsymbol{x}(\cdot)}^* \mathcal{X}$ on $[0, t_f]$, satisfying $[\boldsymbol{p}(t), p^0] \neq 0$ for $t \in [0, t_f]$, such that, a.e. on $[0, t_f]$, the followings [Eqs. (1)–(4)] hold,

$$
\begin{cases}
\dfrac{\mathrm{d}}{\mathrm{d}t}\boldsymbol{x}(t) = \dfrac{\partial H(\boldsymbol{x}(t), \boldsymbol{p}(t), u(t))}{\partial \boldsymbol{p}^T}, \\[2mm]
\dfrac{\mathrm{d}}{\mathrm{d}t}\boldsymbol{p}(t) = -\dfrac{\partial H(\boldsymbol{x}(t), \boldsymbol{p}(t), u(t))}{\partial \boldsymbol{x}^T},
\end{cases} \quad t \in [0, t_f] \setminus \{t_m\}, \tag{1}
$$

$$
H(\boldsymbol{x}(t), \boldsymbol{p}(t), u(t)) = \max_{\eta(t) \in [-1,1]} H(\boldsymbol{x}(t), \boldsymbol{p}(t), \eta(t)), \tag{2}
$$

$$
0 \equiv H(\boldsymbol{x}(t), \boldsymbol{p}(t), u(t)), \tag{3}
$$

$$
\begin{cases}
p_x(t_m^+) = p_x(t_m^-) + \lambda_x, \\
p_y(t_m^+) = p_y(t_m^-) + \lambda_y, \\
p_\theta(t_m^+) = p_\theta(t_m^-),
\end{cases} \tag{4}
$$

where

$$
H(\boldsymbol{x}, \boldsymbol{p}, u) = p_x \cos(\theta) + p_y \sin(\theta) + p_\theta u / \rho + p^0
$$

is the Hamiltonian and λ_x and λ_y are two constants. Note that p_θ and the Hamiltonian H are continuous at t_m because the heading angle and the time at $\boldsymbol{z}_m$ are not fixed (Bryson & Ho, 1969, Section 3.5). As abnormal solutions ($p^0 = 0$) are covered by normal solutions ($p^0 \neq 0$) (Yalcin Kaya, 2017), we shall only consider the case of $p^0 < 0$. Then, the pair $(\boldsymbol{p}, p^0)$ is normalized so that $p^0 = -1$. Explicitly writing Eq. (1) yields, for $t \in [0, t_f] \setminus \{t_m\}$,

$$
\frac{\mathrm{d}}{\mathrm{d}t}\begin{pmatrix} p_x(t) \\ p_y(t) \\ p_\theta(t) \end{pmatrix} = \begin{pmatrix} 0 \\ 0 \\ p_x(t)\sin[\theta(t)] - p_y(t)\cos[\theta(t)] \end{pmatrix}, \tag{5}
$$

implying that p_x and p_y are piecewise constant and

$$
p_\theta = \begin{cases} p_{x_0} y - p_{y_0} x + c_1, \ t \in [0, t_m), \\ (p_{x_0} + \lambda_x) y - (p_{y_0} + \lambda_y) x + c_2, \ t \in (t_m, t_f], \end{cases} \tag{6}
$$

where c_1 and c_2 are two constants and p_{x_0} and p_{y_0} are the values of $p_x(\cdot)$ and $p_y(\cdot)$ on $[0, t_m)$, respectively.

According to Eq. (6), if $p_\theta(\cdot) \equiv 0$ on a nonzero interval $[t_1, t_2] \subset [t_0, t_f]$, the graph of $(x(\cdot), y(\cdot))$ on $[t_1, t_2]$ forms a straight line segment, indicating $u(\cdot) \equiv 0$ on this interval. Thus, in view of Eq. (2), the switching of u is totally determined by p_θ, i.e.,

$$
u = \begin{cases} 1, & p_\theta > 0, \\ 0, & p_\theta \equiv 0, \\ -1, & p_\theta < 0. \end{cases} \tag{7}
$$

In the next section, we shall use the necessary conditions to characterize the solution of 3PDP.

3. Characterization of the solution of 3PDP

Denote by "S" and "C" a straight line segment and a circular arc with a radius of ρ, respectively. According to Dubins (1957) and Sussmann and Tang (1994), the shortest Dubins path between two configurations is of type CCC or CSC or a substring thereof. Furthermore, if denoting by R (resp. L) the corresponding circular arc with a right (resp. left) turning direction, we have

- CCC = {RLR, LRL}, and
- CSC = {RSR, RSL, LSL, LSR}.

According to Bellman's principle for optimality, the solution of 3PDP can be concatenated by CCC and CSC so that it belongs to 36 types:

CCC|CCC, CCC|CSC, CSC|CCC, CSC|CSC,

or substrings thereof where the words before and after "|" denote the types before and after $\boldsymbol{z}_m$, respectively.

3.1. Geometric properties for the solution of 3PDP

For notational simplicity, denote the centers of the right and left circles tangent to the velocity at $\boldsymbol{z}_i$ ($i = 1, 2, m$), respectively, by

$$
\boldsymbol{c}_i^r := \boldsymbol{z}_i + \rho \begin{bmatrix} \sin\theta_i \\ -\cos\theta_i \end{bmatrix} \quad \text{and} \quad \boldsymbol{c}_i^l := \boldsymbol{z}_i - \rho \begin{bmatrix} \sin\theta_i \\ -\cos\theta_i \end{bmatrix}.
$$

Lemma 1. Let $C_1 C_2 C_3$ be the type of a Dubins path between $(\boldsymbol{z}_1, \theta_1)$ and $(\boldsymbol{z}_m, \theta_m)$ such that none of its subarcs vanishes. If $p_\theta(t_m) = 0$ and $\|\boldsymbol{z}_m - \boldsymbol{c}_1^\mu\| \leq \rho$ for either $\mu = r$ or l, the Dubins path is not the shortest between $(\boldsymbol{z}_1, \theta_1)$ and $(\boldsymbol{z}_m, \theta_m)$.

Proof. By contradiction, assume the Dubins path is the shortest. Then, Eqs. (6) and (7) are satisfied. If A and B are the initial and terminal points of C_2, we have $p_\theta = 0$ at A and B because p_θ changes its sign at A and B [cf. Eq. (7)]. As $p_\theta(t_m) = 0$, it follows that A, B, and $\boldsymbol{z}_m$ lie on a straight line according to Eq. (6). However, if none subarcs of $C_1 C_2 C_3$ disappears, A, B, and $\boldsymbol{z}_m$ cannot be on a straight line, completing the proof by contraposition. □

Lemma 2. Let CSC be the type of a Dubins path between $(\boldsymbol{z}_1, \theta_1)$ and $(\boldsymbol{z}_m, \theta_m)$ such that none of its subarcs vanishes. If $p_\theta(t_m) = 0$, the Dubins path is not the shortest between $(\boldsymbol{z}_1, \theta_1)$ and $(\boldsymbol{z}_m, \theta_m)$.

Proof. By contraposition, assume the Dubins path is the shortest. Then, Eqs. (6) and (7) are satisfied. Eq. (7) means $p_\theta = 0$ along the straight line segment S. Since $p_\theta(t_m) = 0$, it follows that $\boldsymbol{z}_m$ lies on S according to Eq. (6), indicating the final circular arc disappears. This contradicts with the lemma's assumption, completing the proof. □

Theorem 1. Let $C_1 T_2 C_3 | C_4 T_5 C_6$ ($T \in \{S, C\}$) be the type of the shortest path of 3PDP. If none of its subarcs vanishes, C_3 and C_4 have the same turning direction.

Proof. By contradiction, assume C_3 and C_4 have different turning directions. Under this assumption, p_θ changes its sign at t_m according to Eq. (7), indicating $p_\theta(t_m) = 0$ as p_θ is continuous according to Eq. (4).

If $T_2 = S$ (resp. $T_5 = S$), Lemma 2 indicates that $C_1 T_2 C_3$ (resp. $C_4 T_5 C_6$) is not the shortest path between $(\boldsymbol{z}_1, \theta_1)$ and $(\boldsymbol{z}_m, \theta_m)$ [resp. $(\boldsymbol{z}_m, \theta_m)$ and $(\boldsymbol{z}_2, \theta_2)$]. This contradicts with the assumption that the path $C_1 T_2 C_3 | C_4 T_5 C_6$ is the shortest, indicating that C_3 and C_4 have the same turning direction by contraposition.

From now on, we consider that $T_2 = C$ and $T_5 = C$. According to Lemma 1 and Bellman's principle, if $\|\boldsymbol{z}_m - \boldsymbol{c}_1^\mu\| \leq \rho$ for either $\mu = r$ or l, the path $C_1 T_2 C_3 | C_4 T_5 C_6$ is not optimal, contradicting with the assumption of this theorem. Hence, if $\|\boldsymbol{z}_m - \boldsymbol{c}_1^\mu\| \leq \rho$ for either $\mu = r$ or l, C_3 and C_4 have the same turning direction. Next, we consider the rest case that $\|\boldsymbol{z}_m - \boldsymbol{c}_1^\mu\| > \rho$ for $\mu \in \{r, l\}$. We first tackle the case that $T_2 = R$ and $T_5 = L$, as illustrated in Fig. 1. Let $\beta > 0$ and $\gamma > 0$ be the radians of T_2 and C_3, respectively. We have $\beta = \gamma$ since the three points A, B, and $\boldsymbol{z}_m$ lie on a straight line ($p_\theta = 0$ at A, B, and $\boldsymbol{z}_m$). According to Bui, Souères, Boissonnat, and Laumond (1994, Lemma 3), we also have $\beta \in (\pi, 2\pi)$. Let $\hat{\beta} > 0$ and $\hat{\gamma} > 0$ be the radians of T_5 and
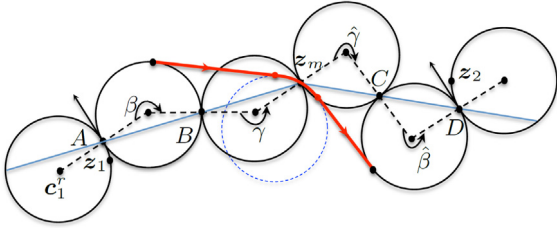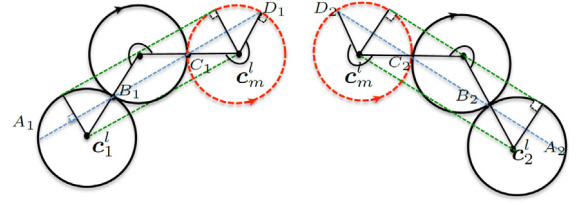
Fig. 1. Geometry for the path of type LRL|RLR.

Fig. 2. Geometry for the type of LRLRL where the two dashed circles are the same one.

C_4, respectively. Analogously, we have $\hat{\beta} = \hat{\gamma} \in (\pi, 2\pi)$. As a result, there always exists a path (as shown by the thickest path) shorter than $C_1T_2C_3|C_4T_5C_6$, contradicting with the assumption of this theorem. For the case of $T_2 = L$ and $T_5 = R$, the path of $C_1T_2C_3|C_4T_5C_6$ cannot be the shortest for the same reason, completing the proof. □

Thanks to this theorem, C_3 and C_4 can be written as a single circular arc. So, we have the following result.

Corollary 1. *The solution path of 3PDP must be of a type in $\mathcal{F} = \{CCCCC, CSCCC, CCCSC, CSCSC\}$ or a substring thereof, where*

- CCCCC = $\{$RLRLR, LRLRL$\}$,
- CCCSC = $\{$RLRSR, RLRSL, LRLSL, LRLSR$\}$,
- CSCCC = $\{$RSRLR, LSRLR, RSLRL, LSLRL$\}$,
- CSCSC =$\{$ RSRSR, LSRSR, RSRSL, LSRSL, LSLSL, RSLSL, LSLSR, RSLSR $\}$.

It should be noted that, along the solution paths of the DTSP and the CCSPP, this corollary holds for the pieces of any 3 consecutive points.

3.2. Common formula for the types in $\mathcal{F}$

In this subsection, a common formula is established for all the 18 types in $\mathcal{F}$ by the following theorem.

Theorem 2. *Let $C_1T_2C_3T_4C_5$ ($T \in \{S, C\}$) be the type of the solution path of 3PDP so that none of its subarcs vanishes, we have*

$$\frac{\cos(\phi_1 - \theta_m)}{\cos(\alpha_1/2)} = \frac{\cos(\phi_2 - \theta_m)}{\cos(\alpha_2/2)}, \tag{8}$$

where

(a) *if $T_2 = S$, then $\alpha_1 = 0$ and $\phi_1 \in [0, 2\pi)$ is the orientation angle of the line segment T_2;*

(b) *if $T_2 = C$, then $\alpha_1 \in (\pi, 2\pi)$ is the radian of T_2 such that $\cos(\alpha_1) = (8\rho^2 - \|\boldsymbol{c}_m^\mu - \boldsymbol{c}_1^\mu\|^2)/8\rho^2$ and $\phi_1 \in [0, 2\pi)$ is the orientation angle of the vector $\boldsymbol{c}_m^\mu - \boldsymbol{c}_1^\mu$ where $\mu = r$ if $T_2 = L$ and $\mu = l$ otherwise;*

(c) *if $T_4 = S$, then $\alpha_2 = 0$ and $\phi_2 \in [0, 2\pi)$ is the orientation angle of the line segment T_4; and*

(d) *if $T_4 = C$, then $\alpha_2 \in (\pi, 2\pi)$ is the radian of T_4 such that $\cos(\alpha_2) = (8\rho^2 - \|\boldsymbol{c}_2^\mu - \boldsymbol{c}_m^\mu\|^2)/8\rho^2$ and $\phi_2 \in [0, 2\pi)$ is the orientation angle of the vector $\boldsymbol{c}_2^\mu - \boldsymbol{c}_m^\mu$ where $\mu = r$ if $T_4 = L$ and $\mu = l$ otherwise.*

Proof. We first tackle the case of $T_2 = T_4 = R$. The proof will be based on the geometry in Fig. 2. Let $\alpha_1 > 0$ and $\beta_1 \in [0, 2\pi)$ be the radian of T_2 and the HOA at the point B_1, respectively. It follows from Bui et al. (1994, Lemma 3) that $\alpha_1 \in (\pi, 2\pi)$. Since $p_\theta = 0$ and $H = 0$ at B_1 and C_1, it follows

$$p_{x_0} \cos \beta_1 + p_{y_0} \sin \beta_1 - 1 = 0, \tag{9}$$

$$p_{x_0} \cos \gamma_1 + p_{y_0} \sin \gamma_1 - 1 = 0,$$

where $\gamma_1 = \beta_1 - \alpha_1$ is the HOA at C_1. Combining these two equations by the trigonometric sum-to-product formulas yields

$$0 = (p_{x_0} \sin \frac{\beta_1 + \gamma_1}{2} - p_{y_0} \cos \frac{\beta_1 + \gamma_1}{2}) \sin \frac{\alpha_1}{2}.$$

Since $\sin(\alpha_1/2) \neq 0$ due to $\alpha_1 \in (\pi, 2\pi)$, it follows

$$p_{x_0} \sin[(\beta_1 + \gamma_1)/2] - p_{y_0} \cos[(\beta_1 + \gamma_1)/2] = 0. \tag{10}$$

Let $\beta_2 \in [0, 2\pi)$ and $\alpha_2 >$ be the HOA at B_2 and the radian of T_4, respectively. Analogously, we have $\alpha_2 \in (\pi, 2\pi)$ and

$$(p_{x_0} + \lambda_x) \cos \beta_2 + (p_{y_0} + \lambda_y) \sin \beta_2 - 1 = 0, \tag{11}$$

$$(p_{x_0} + \lambda_x) \cos \gamma_2 + (p_{y_0} + \lambda_y) \sin \gamma_2 - 1 = 0,$$

where $\gamma_2 = \beta_2 + \alpha_2$ is the HOA at C_2, indicating

$$0 = (p_{x_0} + \lambda_x) \sin \frac{\beta_2 + \gamma_2}{2} - (p_{y_0} + \lambda_y) \cos \frac{\beta_2 + \gamma_2}{2}. \tag{12}$$

Also notice that $\phi_1 := (\beta_1 + \gamma_1)/2 = \beta_1 - \alpha_1/2$ is the orientation angle of the vector $\boldsymbol{c}_m^l - \boldsymbol{c}_1^l$, and that $\phi_2 := (\beta_2 + \gamma_2)/2 = \beta_2 + \alpha_2/2$ is the orientation angle of the vector $\boldsymbol{c}_2^l - \boldsymbol{c}_m^l$. At $\boldsymbol{z}_m$, the switching function $p_\theta(\cdot)$ and the Hamiltonian function are continuous, implying

$$\lambda_x \cos \theta_m + \lambda_y \sin \theta_m = 0. \tag{13}$$

Let $\psi_1 \in [0, 2\pi)$ and $\psi_2 \in [0, 2\pi)$ be two angles such that

$$\cos(\psi_1) = p_{x_0}/\sqrt{p_{x_0}^2 + p_{y_0}^2}, \quad \sin(\psi_1) = p_{y_0}/\sqrt{p_{x_0}^2 + p_{y_0}^2},$$

and

$$\sin(\psi_2) = \lambda_x/\sqrt{\lambda_x^2 + \lambda_y^2}, \quad \cos(\psi_2) = \lambda_y/\sqrt{\lambda_x^2 + \lambda_y^2}.$$

Then, Eqs. (9)–(12) are, respectively, written as

$$1 = \sqrt{p_{x_0}^2 + p_{y_0}^2} \cos(\beta_1 - \psi_1), \tag{14}$$

$$0 = \sqrt{p_{x_0}^2 + p_{y_0}^2} \sin(\phi_1 - \psi_1), \tag{15}$$

$$1 = \sqrt{p_{x_0}^2 + p_{y_0}^2} \cos(\beta_2 - \psi_1) + \sqrt{\lambda_x^2 + \lambda_y^2} \sin(\beta_2 + \psi_2), \tag{16}$$

$$0 = \sqrt{p_{x_0}^2 + p_{y_0}^2} \sin(\phi_2 - \psi_1) - \sqrt{\lambda_x^2 + \lambda_y^2} \cos(\phi_2 + \psi_2). \tag{17}$$

Combining Eq. (16) with Eq. (17) leads to

$$\cos(\phi_2 + \psi_2) = \sqrt{p_{x_0}^2 + p_{y_0}^2} \big[\cos(\beta_2 - \psi_1) \cos(\phi_2 + \psi_2) + \sin(\beta_2 + \psi_2) \sin(\phi_2 - \psi_1)\big].$$

Substituting Eq. (14) into this equation yields

$$\cos(\phi_2 + \psi_2) \cos(\beta_1 - \psi_1) = \cos(\beta_2 - \psi_1) \cos(\phi_2 + \psi_2) + \sin(\beta_2 + \psi_2) \sin(\phi_2 - \psi_1).$$

Using the trigonometric product-to-sum formulas, this equation is reduced to

$$\cos(\phi_2 + \psi_2)\cos(\beta_1 - \psi_1) = \frac{1}{2}\big[\cos(\beta_2 - \psi_1 - \psi_2 - \phi_2)$$
$$+ \cos(\beta_2 + \psi_2 + \psi_1 - \phi_2)\big].$$

Reversely, using the trigonometric sum-to-product formulas, we eventually obtain

$$\cos(\beta_2 - \phi_2)\cos(\psi_1 + \psi_2) = \cos(\phi_2 + \psi_2)\cos(\beta_1 - \psi_1).$$

Note that $p_\theta = p_{x_0}y - p_{y_0}x + c_1 \equiv 0$ along the straight line connecting B_1 and C_1. Because of the definition of ψ_1 and the fact that the vector $\mathbf{c}_m^l - \mathbf{c}_1^l$ is align with the straight line connecting B_1 and C_1, we have $\psi_1 = \phi_1$. By Eq. (13) and the definition of ψ_2, we have $\psi_2 = -\theta_m + k\pi$. According to the law of cosines in trigonometry and the geometry in Fig. 2, we have

$$\cos(\alpha_i) = (8\rho^2 - \|\mathbf{c}_i^\mu - \mathbf{c}_m^\mu\|^2)/8\rho^2, \quad i = 1, 2.$$

Up to now, we have proven that Eq. (8) holds for $T_2 = T_4 = R$. Based on the same idea, we can prove that Eq. (8) holds for $T_2 = T_4 = L$.

Note that the path of $T_2 = S$ is the limit case of $T_2 = C$ by considering that the radius of the circular arc is infinite. Hence, according to the above analyses, if $T_2 = S$, we have $\beta_1 = \gamma_1 = \phi_1$, indicating $\alpha_1 = 0$ and ϕ_1 is the orientation angle of the straight line. Analogously, if $T_4 = S$, we have $\beta_2 = \gamma_2 = \phi_2$, indicating $\alpha_2 = 0$ and ϕ_2 is the orientation angle of the straight line, completing the proof. $\square$

Remark 1. The formula in Eq. (8) gives the relationship between the unknown θ_m and known parameters: $(\mathbf{z}_1, \theta_1)$, $(\mathbf{z}_2, \theta_2)$, $\mathbf{z}_m$, and ρ. To our best knowledge, the formula in Eq. (8) holding for such a general 3PDP does not exist in the literature. This formula indicates followings:

- If the path of 3PDP is of type CSC_mSC, according to the proof of Theorem 2 we have $p_{x_0} = \cos\phi_1$, $p_{y_0} = \sin\phi_1$, $p_{x_0} + \lambda_x = \cos\phi_2$, and $p_{y_0} + \lambda_y = \sin\phi_2$. Combining these equations with Eq. (13) yields $\tan\theta_m = \tan[(\phi_1 + \phi_2)/2]$, indicating that the mid point $\mathbf{z}_m$ bisects the circular arc C_m. This rules out the possibility that the radian of C_m may be 2π, stated in Goaoc et al. (2013).
- It is worth mentioning that, assuming $\|\mathbf{z}_1 - \mathbf{z}_m\| \geq 4\rho$ and $\|\mathbf{z}_2 - \mathbf{z}_m\| \geq 4\rho$, some formulas in terms of θ_m and known parameters: $(\mathbf{z}_1, \theta_1)$, $(\mathbf{z}_2, \theta_2)$, $\mathbf{z}_m$, and ρ were presented in Sadeghi and Smith (2016) by inverse geometry. If the path type is CSCSC, by some simple algebraic operations, it can be shown that the results in Sadeghi and Smith (2016) are equivalent with Eq. (8), but the results in Sadeghi and Smith (2016) does not apply if the path is not CSCSC.

With the exception of θ_m, all other variables in Eq. (8) are some algebraic combinations of $(\mathbf{z}_1, \theta_1)$, $\mathbf{z}_m$, $(\mathbf{z}_2, \theta_2)$, and ρ. Hence, it is enough to find the zeros of Eq. (8) in order to solve the 3PDP. However, a nonlinear equation may have multiple roots and a numerical solver may not find all those roots. In the subsequent section, we shall show that the formula can be converted into polynomials so that multiple roots can be computed by a standard polynomial solver.

4. Polynomial-based solution for 3PDP

For each type in $\mathcal{F}$, the formula in Eq. (8) can be written as multivariable polynomials in terms of $\sin\theta_m$ and $\cos\theta_m$. Hence, by substituting the half-angle formulas

$$\sin\theta = \frac{2\tan(\frac{\theta}{2})}{1 + \tan^2(\frac{\theta}{2})} \text{ and } \cos\theta = \frac{1 - \tan^2(\frac{\theta}{2})}{1 + \tan^2(\frac{\theta}{2})} \quad (18)$$

Table 1
The degree of polynomial for each type in $\mathcal{F}$.

Degree	Type
4	LSLSL, RSRSR
6	RLRLR, LRLRL
8	{CSCSC}\{RSRSR,LSLSL}, RLRSR, RSRLR, LSLRL, LRLSL
20	RLRSL, LSRLR, LRLSR, RSLRL

into Eq. (8), one obtains a polynomial in terms of $\tan(\theta_m/2)$ and the coefficients of the polynomial are combinations of known variables: $\mathbf{z}_1$, $\mathbf{z}_m$, $\mathbf{z}_2$, θ_1, θ_2, and ρ. The resulting polynomial can be solved by a standard polynomial solver to obtain $\tan(\theta_m/2)$. (Thanks to the development of the QR algorithm for finding matrix eigenvalues, the problem of polynomial zero finding can be solved efficiently in general (Higham, 2002, p. 94)). Since the conversion of Eq. (8) into polynomials is elementary but overlong, we present below a representative example to show the core idea.

Example 1 (*The Polynomial for RSRLR*). If the path of 3PDP is of type RSRLR, Theorem 2 indicates $\alpha_1 = 0$, $\cos(\phi_1 - \theta_m) = \frac{(\cos\theta_m, \sin\theta_m)(\mathbf{c}_m^r - \mathbf{c}_1^r)}{\|\mathbf{c}_m^r - \mathbf{c}_1^r\|}$, and $\cos(\phi_2 - \theta_m) = \frac{(\cos\theta_m, \sin\theta_m)(\mathbf{c}_2^r - \mathbf{c}_m^r)}{\|\mathbf{c}_2^r - \mathbf{c}_m^r\|}$. Substituting these equations into Eq. (8) and squaring the result yield

$$0 = [(\cos\theta_m, \sin\theta_m)(\mathbf{c}_2^r - \mathbf{c}_m^r)]^2/\|\mathbf{c}_2^r - \mathbf{c}_m^r\|^2 \cos^2(\alpha_2/2)$$
$$- [(\cos\theta_m, \sin\theta_m)(\mathbf{c}_m^r - \mathbf{c}_1^r)]^2/\|\mathbf{c}_m^r - \mathbf{c}_1^r\|^2, \quad (19)$$

where $\cos^2(\alpha_2/2) = (\cos\alpha_2 + 1)/2 = (16\rho^2 - \|\mathbf{c}_2^r - \mathbf{c}_m^r\|^2)/16\rho^2$. Then, substituting the explicit expressions of $\mathbf{c}_1^r, \mathbf{c}_2^r, \mathbf{c}_m^r$ into the equation, we get

$$0 = A_1 \cos^4\theta_m + A_2 \cos^3\theta_m \sin\theta_m + A_3 \cos^3\theta_m$$
$$+ A_4 \cos^2\theta_m \sin\theta_m + A_5 \cos^2\theta_m + A_6 \cos\theta_m \sin\theta_m$$
$$+ A_7 \cos\theta_m + A_8 \sin\theta_m + A_9, \quad (20)$$

where A_1–A_9 are constant combinations of $\mathbf{z}_1$, $\mathbf{z}_2$, $\mathbf{z}_m$, θ_1, θ_2, and ρ. Once we substitute Eq. (18) into Eq. (20), we finally obtain

$$0 = B_1 \tan^8(\theta_m/2) + B_2 \tan^7(\theta_m/2) + B_3 \tan^6(\theta_m/2)$$
$$+ B_4 \tan^5(\theta_m/2) + B_5 \tan^4(\theta_m/2) + B_6 \tan^3(\theta_m/2)$$
$$+ B_7 \tan^2(\theta_m/2) + B_8 \tan(\theta_m/2) + B_9,$$

where B_1–B_9 are constant combinations of A_1–A_9.

This example shows the corresponding polynomial for RSRLR is of degree 8. Following the same idea as applied in Example 1, one obtains the degrees of polynomials for other types in $\mathcal{F}$, presented in Table 1. While the degrees of polynomials for four types in $\mathcal{F}$ are up to 20, those for the rest in $\mathcal{F}$ are not more than 8. In fact, a polynomial with a degree no more than 20 can be solved efficiently. (As shown by the numerical simulations in Section 5, the time for computing a polynomial with its degree no more than 20 is less than the time for computing a Dubins path between two configurations.)

Recall that the formula in (8) holds as long as none of subarcs of the types in $\mathcal{F}$ vanishes. By the following lemma, the value of θ_m can be readily obtained even if one or more subarcs disappear.

Lemma 3. Let $\mathcal{T}$ be the type of the shortest Dubins path between two configurations $(\mathbf{y}_1, \eta_1)$ and $(\mathbf{y}_2, \eta_2)$ in $\mathcal{X}$. For $i = 1$ and 2, denoting the centers of the right and left circles tangent to $(\mathbf{y}_i, \eta_i)$ by

$$\mathbf{c}_{\mathbf{y}_i}^r = \mathbf{y}_i + \rho\begin{pmatrix} \sin\eta_i \\ -\cos\eta_i \end{pmatrix} \text{ and } \mathbf{c}_{\mathbf{y}_i}^l = \mathbf{y}_i - \rho\begin{pmatrix} \sin\eta_i \\ -\cos\eta_i \end{pmatrix}$$

respectively, the following statements hold:

(a) If $\mathcal{T} = S$, then $\eta_1 = \eta_2$.

(b) If $\mathcal{T} = CC$, then we have

$$\begin{cases} \|\boldsymbol{c}_{\boldsymbol{y}_1}^r - \boldsymbol{c}_{\boldsymbol{y}_2}^l\| = 2\rho, & \mathcal{T} = RL, \\ \|\boldsymbol{c}_{\boldsymbol{y}_1}^l - \boldsymbol{c}_{\boldsymbol{y}_2}^r\| = 2\rho, & \mathcal{T} = LR. \end{cases}$$

(c) If $\mathcal{T} = C$, then

$$\begin{cases} \boldsymbol{c}_{\boldsymbol{y}_1}^r = \boldsymbol{c}_{\boldsymbol{y}_2}^r, & \mathcal{T} = R \\ \boldsymbol{c}_{\boldsymbol{y}_1}^l = \boldsymbol{c}_{\boldsymbol{y}_2}^l, & \mathcal{T} = L \end{cases}$$

(d) If $\mathcal{T} = CS$, then we have

$$\begin{cases} (\sin \eta_2, -\cos \eta_2)(\boldsymbol{c}_{\boldsymbol{y}_1}^r - \boldsymbol{y}_2) = \rho, & \mathcal{T} = RS \\ (-\sin \eta_2, \cos \eta_2)(\boldsymbol{c}_{\boldsymbol{y}_1}^l - \boldsymbol{y}_2) = \rho, & \mathcal{T} = LS \end{cases}$$

(e) If $\mathcal{T} = SC$, then we have

$$\begin{cases} (-\sin \eta_1, \cos \eta_1)(\boldsymbol{c}_{\boldsymbol{y}_2}^r - \boldsymbol{y}_1) = \rho, & \mathcal{T} = SR \\ (\sin \eta_1, -\cos \eta_1)(\boldsymbol{c}_{\boldsymbol{y}_2}^l - \boldsymbol{y}_1) = \rho, & \mathcal{T} = SL. \end{cases}$$

Proof. The proofs for (a), (b), and (c) are trivial. For (d), we handle the case of $\mathcal{T} = RS$. Let $\boldsymbol{e} = (\sin \eta_2, -\cos \eta_2)$. Then, we have $(\boldsymbol{c}_{\boldsymbol{y}_1}^r - \rho \boldsymbol{e} - \boldsymbol{y}_2)^T \boldsymbol{e} = 0$, proving the first case of (d). Note that (e) and the second case of (d) can be proved in the same way, completing the proof. □

Once the solution path of 3PDP either before or after $\boldsymbol{z}_m$ has one or more subarcs disappearing, one can have θ_m by solving a corresponding equation in Lemma 3. By combining Lemma 3 and Eq. (8), we present below a Polynomial-Based Method (PBM) to solve the 3PDP.

Given a 3PDP, set $K = \{0, 1, \ldots, 18\}$ and $i = 0$. The PBM is performed by the following steps:

1. By solving the equations in Lemma 3, we can get the HOAs at $\boldsymbol{z}_m$ for all the substrings of the 18 types in $\mathcal{F}$. Let θ_0 be the HOA among the computed HOAs so that the substring is the shortest and let $\mathcal{T}_0$ be the type of the shortest substring. Set $i = i + 1$.

2. Let $\mathcal{T}_j$'s (j = 1,...,18) be the 18 types in $\mathcal{F}$.

    2.1 If $i \leq 18$, go to step 2.2; otherwise go to step 3.

    2.2 use a polynomial solver to find the zeros of the polynomial corresponding to $\mathcal{T}_i$, and denote by $\mathcal{Z}$ the set of real roots;

    2.3 $\Theta = \{\theta \in [0, 2\pi) : \theta = 2 \arctan(z), z \in \mathcal{Z}\}$; if $\Theta = \emptyset$, set $K = K \setminus \{i\}$; otherwise set $\theta_i = \underset{\theta \in \Theta}{\operatorname{argmin}} F[(\boldsymbol{z}_1, \theta_1), (\boldsymbol{z}_m, \theta)] + F[(\boldsymbol{z}_m, \theta), (\boldsymbol{z}_2, \theta_2)]$;

    2.4 set $i = i + 1$ and go to step 2.1;

3. Set

$$I = \underset{i \in K}{\operatorname{argmin}} F[(\boldsymbol{z}_1, \theta_1), (\boldsymbol{z}_m, \theta_i)] + F[(\boldsymbol{z}_m, \theta_i), (\boldsymbol{z}_2, \theta_2)].$$

Then, $\theta_m = \theta_I$ and the shortest path is of type $\mathcal{T}_I$.

With this procedure, one can obtain θ_m for any 3PDP no matter its solution path is of a type in $\mathcal{F}$ or a substring thereof.

Table 2
The average time to solve polynomials with degrees in {4, 6, 8, 20}.

Degree	4	6	8	20
Time (μs)	501.13	524.06	608.28	1317.7

Table 3
The time consumption of PBM compared to DBM(360).

d_m	$> 4\rho$	$= 3\rho$	$= 2\rho$	$= \rho$	$< \rho$
Factor	45.69	24.36	27.19	32.66	36.98

5. Numerical simulations

A straightforward idea to solve the 3PDP is to discretize the HOA at $\boldsymbol{z}_m$ over $[0, 2\pi)$ and to select an angle among the discretized values so that the corresponding path is the shortest. We call this method the Discretization-Based Method (DBM), and we denote by DBM(l) the DBM with a discretization level of $l \in \mathbb{N}$, performed as

$$\theta_m = \underset{\theta \in \Theta}{\operatorname{argmin}} F[(\boldsymbol{z}_1, \theta_1), (\boldsymbol{z}_m, \theta)] + F[(\boldsymbol{z}_m, \theta), (\boldsymbol{z}_2, \theta_2)],$$

where $\Theta = \{2(i-1)\pi/l : i = 1, \ldots, l\}$. In this section, we shall present some numerical simulations to show the performance of PBM in comparison with DBM.

5.1. Computational complexity

Through a large number of simulations, the time of solving a polynomial (with a degree in {4, 6, 8, 20}) by the method of finding the eigenvalues of a characteristic matrix corresponding to each polynomial is tested by MATLAB on a desktop with Intel(R) Core(TM) i7-3615QM CPU @2.30 GHz and shown in Table 2, where the unit of time is microsecond (μs). Additional simulations on the same desktop show that the time of solving a Dubins problem between two configurations is around 4020.9 μs. It is clear that solving a polynomial with a degree in {4, 6, 8, 20} requires less time than solving a Dubins problem. Therefore, the time for solving corresponding polynomials just slightly increases the total time complexity of the PBM, and the PBM is much more efficient than the DBM, as shown by the simulations discussed in the next paragraph.

Let the parameters $(\boldsymbol{z}_1, \theta_1)$, $(\boldsymbol{z}_2, \theta_2)$, and $\boldsymbol{z}_m$ be generated randomly by uniform distribution; both the DBM(360) and the PBM are tested on 10000 randomly generated 3PDPs. If $d_m \in \mathbb{R}_+$ is the minimum distance between two consecutive points of 3PDP, Table 3 shows the improvement factors of the PBM compared with the DBM(360) for different values of d_m. Notice that the improvement factor for $d_m > 4\rho$ is the largest since in this case only the type of CSCSC needs to be checked. In the case of $d_m < \rho$, some types of CSCSC are ruled out so that only partial types in $\mathcal{F}$ are required to check, resulting in a larger improvement factor in comparison with $d_m = 3\rho$, 2ρ, and ρ. It is worth remarking that an iterative method was proposed in Sadeghi and Smith (2016) to solve the 3PDP; although the improvement factor of the iterative method is around 13.6 for $d_m = 4\rho$, they are just around 6.8 and 5.2 when d_m equals 3ρ and 2ρ, respectively. In fact, the iterative method does not apply unless the path is of type CSCSC. To this end, the PBM is not only more efficient but also able to handle more general cases than the iterative method.

5.2. Accuracy

In this subsection, we present two specific examples (case A and case B) to show the performance of the PBM.
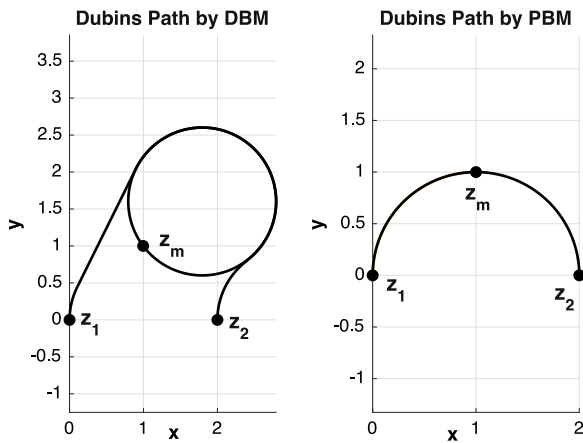
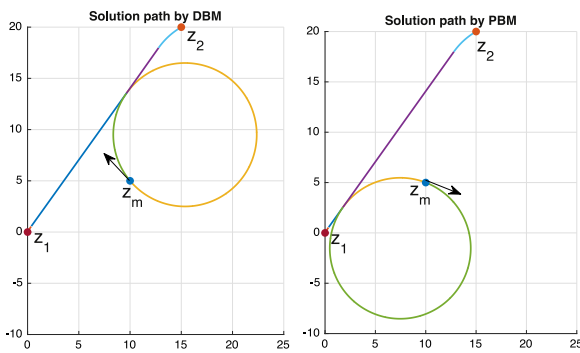**Fig. 3.** Case A: the solution paths of the 3PDP computed by PBM and DBM(360).

Fig. 4. Case B: the solution paths of the 3PDP computed by PBM and DBM(360).

5.2.1. Case A

The parameters of the 3PDP are given by $(\boldsymbol{z}_1, \theta_1) = (0, 0, \pi/2)$, $\boldsymbol{z}_m = (1 + \cos(91.25 * \pi/180), \sin(91.25 * \pi/180))$, $(\boldsymbol{z}_2, \theta_2) = (2, 0, -\pi/2)$, and $\rho = 1$. These parameters are tailored so that the shortest path is a half circle (as shown by the right picture in Fig. 3) and $\theta_m = 1.25$ deg. However, the DBM(360) will never reach this angle so that it finds a non-optimal path, as reported by the left picture in Fig. 3. Note that the optimal angle $\theta_m = 1.25$ deg can be reached if $l \geq 1440$, which however results in a higher computational complexity.

5.2.2. Case B

We consider an example pointed out by an anonymous referee. The parameters are given by $(\boldsymbol{z}_1, \theta_1) = (0, 0, 60 \text{ deg})$, $\boldsymbol{z}_m = (10, 5)$, and $(\boldsymbol{z}_2, \theta_2) = (15, 20, 30 \text{ deg})$. The solution is computed by PBM and DBM(360) for different minimum turning radius in $[1, 10]$, showing that the length of solution computed by PBM is always slightly less than that by DBM (360). (This is reasonable since the PBM leads to more accurate results.) However, we find that when $\rho \in [7, 8]$, the geometries of solutions are different as shown by Fig. 4 where $\rho = 7$. Numerical simulation shows that the geometries will be the same unless $l \geq 26000$, which means the DBM(l) requires more computation time than the PBM in order to achieve the same geometry.

6. Conclusions

In this paper, the solution of 3PDP was studied without any restriction and assumption. Though a direct application of Bellman's principle of optimality indicates that the solution of 3PDP should be among 36 types or their substrings, a study on the necessary conditions led us to reduce the number of types to 18. As a consequence, solving any 3PDP amounts to checking at most 18 types or their substrings. While the length of each substring could be readily checked (cf. Lemma 3), a formula for the 18 types was established. This formula revealed the relationship between the unknown HOA at mid point and known parameters of the 3PDP. Further analyses on the formula showed that it could be converted into some polynomials with degrees of at most 20. Thus, an efficient PBM was proposed to solve the 3PDP. Numerical simulations showed that the PBM was superior compared with the straightforward DBM. It is worth mentioning that the results of this paper allow to improve the performance of some existing algorithms for solving the CCSPP, which is a foundational problem in the field of motion planning.

References

Arora, S. (1998). Polynomial time approximation schemes for euclidean traveling salesman and other geometric problems. *Journal of the ACM, 45*(5), 753–782.

Bellman, R. E. (1957). *Dynamic programming.* Princeton, NJ: Princeton University Press.

Bryson, E., & Ho, Y.-C. (1969). *Applied optimal control: Optimization, estimation, and control.* Blaisdell Publishing Company.

Bui, X.-N., Souères, P., Boissonnat, J.-D., & Laumond, J.-P. (1994). Shortest path synthesis for dubins non-holonomic robot. In *1994 IEEE international conference on robotics and automation.* San Diego, CA, USA.

Cohen, I., Epstein, C., Isaiah, P., Kuzi, S., & Shima, T. (2017). Discretization-based and look-ahead algorithms for the dubins traveling salesperson problem. *IEEE Transactions on Automation Science and Engineering, 14*(1), 383–390.

Cohen, I., Epstein, C., & Shima, T. (2017). On the discretized dubins traveling salesman problem. *IISE Transactions, 49*(2), 238–254.

Dubins, L. E. (1957). On curves of minimal length with a constraint on average curvature, and with prescribed initial and terminal positions and tangents. *American Journal of Mathematics, 79*(3), 497–516.

Edison, E., & Shima, T. (2011). Integrated task assignment and path optimization for cooperating uninhabited aerial vehicles using genetic algorithms. *Computers & Operations Research, 38*(1), 340–356.

Goaoc, X., Kim, H.-S., & Lazard, S. (2013). Bounded-curvature shortest paths through a sequence of points using convex optimisation. *SIAM Journal on Computing, 42*(2), 662–684.

Higham, N. (2002). *Accuracy and stability of numerical algorithms* (2nd ed.). Society for Industrial and Applied Mathematics.

Isaiah, P., & Shima, T. (2015). Motion planning algorithms for the dubins traveling salesperson problem. *Automatica, 53*, 247–255.

Lawler, E. L., Lenstra, J. K., Rinnooy Kan, A. H. G., & Shmoys, D. B. (1985). *The traveling salesman problem: A guided tour of combinatorial optimization.* New York: Wiley.

Lee, J.-H., Cheong, O., Kwon, W.-C., Shin, S. Y., & Chwa, K.-Y. (2000). Approximation of curvature-constrained shortest paths through a sequence of points. In M. A. Paterson (Ed.), *Algorithms ESA 2000, 8th annual european symposium* (pp. 314–325). Saarburcken, Germany: Springer-Verlag.

Lugo-Cárdenas, I., Flores, G., Salazar, S., & Lozano, R. (2014). Dubins path generation for a fixed wing uav. In *2014 international conference on unmanned aircraft systems (ICUSA).* Orlando, FL, USA.

Lynch, K. M. (2003). Optimal control of the thrusted skate. *Automatica, 39*(1), 173–176.

Ma, X., & Castanon, D. (2006). Receding horizon planning for dubins traveling salesman problems. In *Proc. IEEE conference on decision and control* (pp. 5453–5458). San Diego, CA, USA.

Matveev, A. S., Teimoori, H., & Savkin, A. V. (2011). A method for guidance and control of an autonomous vehicle in problems border patrolling and obstacle avoidnace. *Automatica, 47*, 515–524.

Ny, J. L., Feron, E., & Frazzoli, E. (2012). On the dubins travelling salesman problem. *IEEE Transactions on Automatic Control, 57*(1), 265–270.

Pontryagin, L. S., Boltyanski, V. G., Gamkrelidze, R. V., & Mishchenko, E. F. (1962). *The mathematical theory of optimal processes (Russian).* English translation: Interscience.

Rathinam, S., & Khargonekar, P. (2016). An approximation algorithm for a shortest dubins path problem. In *ASME 2016 dynamic systems and control conference, number DSCC* (pp. 2016–9798).

Rathinam, S., Sengupta, R., & Darbha, S. (2007). A resource allocation algorithm for multivehicle systems with nonholonomic constraints. *IEEE Transactions on Automation Science and Engineering, 4*(1), 98–104.

Sadeghi, A., & Smith, S. L. (2016). On efficient computation of shortest dubins paths through three consecutive points. In *IEEE 55th conference on decision and control (DCD)*. Las Vegas, USA.

Salva, K., Frazzoli, E., & Bullo, F. (2005). On the point-to-point and travelling salesperson problem for dubins' vehicle. In *American control conference*. Portland, OR.

Sussmann, H. J., & Tang, G. (1994). *Shortest paths for the reeds-shepp car: A worked out example of the use of geometric techniques in nonlinear optimal control. Technical report*. Rutgers University.

Takei, R., & Tsai, R. (2013). Optimal trajectories of curvature constrained motion in the hamilton-jacobi formulation. *Journal of Scientific Computing*, *54*(2–3), 622–644.

Takei, R., Tsai, R., Shen, H., & Landa, Y. (2010). A practical path-planning algorithm for a simple car: A hamilton-jacobi approach. In *American control conference*. Marriott Waterfront, Baltimore, MD, USA.

Tang, Z., & Özgüner, Ü. (2005). Motion planning for multitarget surveillance with mobile sensor agents. *IEEE Transactions on Robotics*, *21*(5), 898–908.

Wright, S. J. (2015). Coordinate descent algorithms. *Mathematical Programming*, *151*(1), 3–24.

Yalcin Kaya, C. (2017). Markov-dubins path via optimal control theory. *Computational Optimization and Applications*, *68*(3), 719–747.

Yu, X., & Hung, J. Y. (2012). A genetic algorithm for the dubins travelling salesman problem. In *IEEE international symposium on industrial elections*. Hangzhou, China.

Zheng Chen received the Ph.D. degree in Applied Mathematics from the University Paris-Saclay in 2016, the M.Sc and B.Sc in Aerospace Engineering from Northwestern Polytechnical University in 2013 and 2010, respectively. From Sept. 2016 to Jul. 2017, he worked as a postdoctoral fellow at the University of Toulouse, and from Sept. 2017 to Dec. 2018, he worked as a postdoctoral fellow at the Technion — Israel Institute of Technology. He is currently a researcher with the School of Aeronautics and Astronautics at Zhejiang University. His research interests revolve around guidance and control in aerospace engineering.

Tal Shima received the Ph.D. degree from the Technion — Israel Institute of Technology, Haifa, Israel, in 2001. He is currently a Professor with the Department of Aerospace Engineering at the Technion. He is the Director and Founder of the Technion's Cooperative Autonomous Systems Laboratory. His current research interests are in the area of guidance of vehicles, in particular missiles and unmanned aircraft, operating individually or as a team. He is an Associate Fellow of AIAA and an Associate Editor for the IEEE Transactions on Aerospace and Electronic Systems and IEEE Transactions on Control Systems Technology.